

# RSC Advances

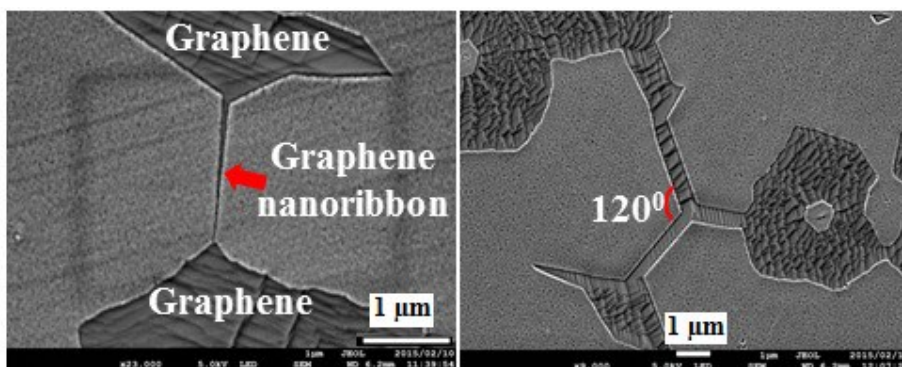


This is an *Accepted Manuscript*, which has been through the Royal Society of Chemistry peer review process and has been accepted for publication.

*Accepted Manuscripts* are published online shortly after acceptance, before technical editing, formatting and proof reading. Using this free service, authors can make their results available to the community, in citable form, before we publish the edited article. This *Accepted Manuscript* will be replaced by the edited, formatted and paginated article as soon as this is available.

You can find more information about *Accepted Manuscripts* in the [Information for Authors](#).

Please note that technical editing may introduce minor changes to the text and/or graphics, which may alter content. The journal's standard [Terms & Conditions](#) and the [Ethical guidelines](#) still apply. In no event shall the Royal Society of Chemistry be held responsible for any errors or omissions in this *Accepted Manuscript* or any consequences arising from the use of any information it contains.



Demonstrated formation of nanoribbons, and Y-junctions structures with controllable hydrogen-induced anisotropic etching of chemical vapor deposited graphene on Cu foil. The distinct graphene edges of individual ribbon created  $120^\circ$  to form a Y-shape structure.

## Formation of graphene nanoribbons and Y-junctions by hydrogen induced anisotropic etching

Remi Papon<sup>1</sup>, Subash Sharma<sup>1</sup>, Sachin M. Shinde<sup>1</sup>, Amutha Thangaraja<sup>1</sup>, Golap Kalita<sup>\*</sup>  
<sup>1,2</sup>, Masaki Tanemura<sup>1</sup>

<sup>1</sup>Department of Frontier Materials, Nagoya Institute of Technology, Gokiso-cho, Showa-ku, Nagoya 466-8555, Japan

<sup>2</sup>Center for Fostering Young and Innovative Researchers, Nagoya Institute of Technology, Gokiso-cho, Showa-ku, Nagoya, 466-8555, Japan

\*Corresponding authors: E-mail: (G.K.) [kalita.golap@nitech.ac.jp](mailto:kalita.golap@nitech.ac.jp); Phone/Fax: +81-52-735-5216

**Keywords:** Graphene, nanoribbons, Y-junction, anisotropic etching, hydrogen

### Abstract:

Metal nanoparticles and H<sub>2</sub> induced etching of graphene are of significant interest to synthesis graphene nanoribbons and various other structures with crystallographically defined edges. Here, we demonstrate a controllable H<sub>2</sub>-induced etching process of graphene crystals to fabricate nanoribbons, and Y-junctions structures with pronounced edges. Individual graphene crystals and a continuous films were grown on Cu foil by

solid source chemical vapor deposition (CVD) technique. The etching behavior of the synthesized graphene was investigated by annealing at 1000 °C in a gas mixture of H<sub>2</sub> and Ar. A highly anisotropic etching creates hexagonal holes, nanoribbons and Y-junction graphene with clear edge structures. The distinct graphene edges of individual ribbon create 120° to form a Y-shape structure. The finding can be significant to fabricate well-defined graphene structures with controlled edges for electronic device applications as well as creating in-plane heterostructures with other two dimensional (2D) materials.

## 1. Introduction

Graphene, the 2D honeycomb crystal of  $sp^2$  hybridized carbon has been extensively explored for electronic device applications since the experimental observation of extraordinary carrier mobility.<sup>1-6</sup> However, one of the most challenging aspects of graphene is modifying the graphene structure to open a band gap for nanoelectronics applications.<sup>7,8</sup> The intrinsic properties of graphene can be tuned to induce a band gap by confining the charge carriers along one direction in the crystallographic plane.<sup>9,10</sup> Hence, it is quite critical to develop high quality graphene nanoribbons to achieve lateral quantum confinement.<sup>9-12</sup> The properties of graphene nanoribbons are sensitive to the width and the crystallographic orientation of the edges.<sup>13</sup> Nanoribbons with armchair edges have a band gap that changes with the width of ribbons, while zigzag edges have magnetically ordered edge states.<sup>14-16</sup> Various top-down and bottom-up approaches have been adopted to obtain graphene nanoribbons and other nanostructures.<sup>17</sup> Graphene nanoribbons have been obtained by molecular assembly, lithography, “unzipping” of carbon nanotubes (CNTs), plasma etching, metal nanoparticles induced etching process etc.<sup>18-27</sup>

Among the top-down etching processes, anisotropic etching is the most fascinating to

obtain graphene with regular, zigzag or armchair edge structures.<sup>26,28</sup> In this prospect, exploring the anisotropic etching behavior of high quality CVD graphene is of great interest to fabricate nanoribbons with distinct edge structure.<sup>29</sup> Creating holes with defined edge structure also provide a platform to fabricate in-plane heterostructure with other 2D materials. Anisotropic etching of graphene basal plane has been explored with metal catalytic nanoparticles in presence of H<sub>2</sub>, selective oxidation, and water vapor at an elevated temperature.<sup>30-34</sup> Recently, anisotropic behavior of H<sub>2</sub> in the formation of graphene domains has been also observed, thereby obtaining pentagonal graphene domains with anisotropic growth and etching process.<sup>35</sup> Highly anisotropy etching of graphene can be achieved owing to significant differences in chemical reactivity of the zigzag and armchair edges. This has open new opportunities to control the structure of high quality exfoliated and CVD graphene in large-area for device integration. Again, fabrication of Y-shaped graphene nanoribbons with well-ordered edges can be significant, which is not yet addressed considerably. Theoretical analysis predicted specific properties of the Y-shaped zigzag graphene nanoribbons structure.<sup>36-40</sup> Formation of Y-shaped graphene nanoribbons by anisotropic etching process will enable to fabricate multi-terminal graphene-based nanoelectronic and spintronic devices.<sup>41,42</sup> However, synthesis of Y-shaped graphene nanoribbons with clear edges is

still a great challenge. Here, we demonstrate that the controlled H<sub>2</sub>-induced anisotropic etching of graphene can produce hexagonal edge holes, nanoribbons and Y-shaped structures.

## 2. Experimental

Graphene was synthesized by a solid source based atmospheric pressure CVD process on Cu foil (Nilaco Corp.) purity of 99.98% as reported previously.<sup>43</sup> We used solid camphor as precursor for the AP-CVD process to synthesize individual graphene crystals. The Cu foil was cleaned in acetone by sonication prior to synthesis. For the synthesis of graphene, the Cu foil was kept inside the high temperature furnace zone and the carbon source material was put in low temperature furnace. The Cu foil was heated up to 1000 °C and annealed for 15 min in 100 standard cubic meter per minute (sccm) of H<sub>2</sub> atmosphere. During the growth process, H<sub>2</sub> quantity was significantly reduced and Ar was introduced in the growth zone along with H<sub>2</sub>. Hydrogen induced etching of synthesized graphene on Cu foil was investigated by annealing the sample at 1000 °C in the Ar and H<sub>2</sub> (98:2 sccm) gas mixture. Synthesized graphene before and after etching was investigated by optical microscopy, Raman, Field-emission scanning electron microscopy (FE-SEM) and Auger electron spectroscopy (AES). Optical microscopy analysis was performed with the digital optical microscope VHX-500 in

reflectance mode with a Moticam 2000 2.0 M pixel camera. Raman analysis was carried out using NRS 3300 laser Raman spectrometer with a laser excitation energy of 532.08 nm. FE-SEM studies were performed with JEOL JSM-7800F using lower electron detector (LED) upper electron detector (UED) and upper secondary electron detector (USD). AES studies were carried out with JAMP-7800 Auger microscope.

### 3. Results and discussion

High quality individual graphene crystals and continuous graphene films were synthesized to investigate the H<sub>2</sub>-induced etching process. Figure 1(a) and (b) shows optical microscope images of graphene crystals grown from a solid camphor precursor in a developed AP-CVD process. The part with bright contrast of the optical images shows the individual graphene crystals. In figure 1(b), the Cu foil was slightly oxidized to clearly observe graphene domains on polycrystalline Cu grain boundaries. Graphene crystal with a size more than 80 μm was obtained in the CVD process. As well as, continuous graphene films were also synthesized with a longer growth duration. In the CVD process, we observed that the vaporization of solid precursor material significantly influences graphene growth process and layer numbers. Figure 1(c) shows a Raman spectra of the synthesized graphene on Cu foil. The graphitic G and second-order 2D Raman peaks were observed around 1589 and 2700 cm<sup>-1</sup>, respectively.

The higher intensity of 2D peak than that of G peak indicates growth of monolayer graphene. Subsequently, the synthesized graphene on Cu foil was annealed in H<sub>2</sub> atmosphere to explore the anisotropic etching properties.

Figure 2(a)-(c) shows optical microscope images of the annealed sample at 1000 °C in an atmosphere of Ar:H<sub>2</sub> gas mixture. We observed significant etching of the graphene and formation of particular structures. Figure 2(a)-(b) shows formation of ribbons like structures as well as hexagonal holes in the graphene crystals with pronounced edges. Figure 2(c) shows an optical image of an etched graphene crystal with formation of a well-defined hexagonal hole with clear edges. The etching reaction is the reverse reaction of graphene growth process, H<sub>2</sub> can react with the carbon atoms of graphene catalyzed by Cu to produce methane. Figure 2(d) shows Raman analysis of the etched graphene sample on partially oxidized Cu foil at two different positions. Graphitic G and second-order 2D Raman peaks were confirmed at the edge of the graphene structure. While, only copper oxide peak is observed in the reddish part of the Cu foil. Etching of graphene was also investigated in only Ar atmosphere, however the particular etching process was not observed. A gas mixture of H<sub>2</sub> and Ar can be the most suitable to achieve controllable graphene etching for fabrication of various novel structures.

FE-SEM analysis was also performed using LED detector at an accelerating voltage of

5kV to analyze the etched graphene crystals. Figure 3(a) shows a low-resolution SEM image of edge graphene, where we can observed various structures with clear edges. Figure 3(b) and (c) show FE-SEM images of individual graphene structures with clear edges etched along straight lines. The etched part of CVD graphene on base Cu foil remain coupled, while the other part is partially oxidized. The high quality characteristic of CVD graphene remains unchanged after the etching process. As shown in the FE-SEM image, formation of edges with  $60^\circ$  and  $120^\circ$  is observed indicating etching along symmetric directions of the graphene lattice. Such type of well-defined structures of graphene has been also obtained by metal nanoparticles assisted etching process. The  $H_2$ -induced etching process also can be an important tool to obtain triangular-shaped and nanoribbons graphene with control of edge structures.

We have analyzed the etching process of CVD graphene on Cu foil. Figure 4(a) shows a FE-SEM taken by the UED detector at an accelerating voltage of 2kV. The FE-SEM image corresponds to back scattered electron (BSE) providing compositional contrast. We observed  $SiO_2$  nanoparticles as bright contrast inside the hole of graphene crystals and etched areas. The  $SiO_2$  particles play a critical role in etching process of graphene crystals on Cu foil. The etching of graphene can initiate at a defect site, which subsequently propagates with Cu acting as a catalyst for hydrogen to react with  $sp^2$

hybridized carbon atoms. We performed elementary mapping analysis of the etched graphene structures on Cu foil after partial oxidation. Figure 4(b)-(d) shows FE-SEM and elementary mapping at that specific area for carbon and oxygen, respectively. The mapping analysis confirms the graphene and etched areas, where we can observe significant differences in carbon and oxygen concentrations. As shown in figure 4(d), the minimum oxygen detected positions are etched graphene structures coupled with the base Cu surface. Figure 4(e) shows a selective AES analysis of the etched graphene structure on Cu foil. The AES analysis also confirms the remaining graphene structures on the Cu foil.

The formation of well-defined various structures was further investigated by FE-SEM. Figure 5(a) shows FE-SEM images of an ordered etched hexagonal hole as well as ribbon like graphene structure on Cu foil. The sharp etched-edges form  $120^\circ$  and thereby creating a hexagonal hole. Similar to the hexagonal hole, the etched edges with  $60^\circ$  can create a triangular hole at the graphene lattice. This can be significant platform to create defined in-plane heterostructures with other 2D materials such as hexagonal boron nitride.<sup>44</sup> This is a significant observation in our experiments to control the size and structure of the graphene enabling defined heterostructure fabrication. The etching constantly enhances with increase in annealing duration and eventually erasing

significant area of graphene on Cu foil. Figure 5(b) shows formation of Y-shape graphene ribbons structure with edge etching from different directions. The perfect edges of individual ribbon create  $120^\circ$  to form an Y-shape structure. Previously, significant efforts have been made to synthesis Y-shape CNTs owing to its unique electrical properties.<sup>45</sup> The three-terminal Y-junction nanotubes exhibits the gating behavior, characteristic of transistors. Similarly, Y-junction graphene nanoribbons with ordered edge structure (zigzag) can be significant for transistor and spintronic applications. However, a control synthesis process of Y-shaped graphene nanoribbons can be challenging. Thus, we demonstrate that the anisotropic etching process is a suitable tool to create Y-shaped graphene nanoribbons, which will enable us to fabricate multi-terminal graphene-based nanoelectronics devices. Figure 5(c) and (d) shows formation of the graphene nanoribbon structure with the etching process. The nanoribbon is formed with interconnection of two larger graphene domains. This type of structure can be directly integrated as source, drain and channel for a transistor fabrication. The width of the ribbon at one end is  $\sim 67.7$  nm, whereas at the other end is around  $\sim 17$  nm. The width of fabricated nanoribbons is not uniform, however fabrication of sub-10 nm ribbon can be possible by the simple etching process. These results show the formation of graphene nanoribbons and possibilities of obtaining Y and

Z-shaped junction structures with control H<sub>2</sub>-induced etching process of the CVD graphene.

#### 4. Conclusions

We have demonstrated a controllable H<sub>2</sub>-induced etching process of CVD synthesized graphene to fabricate nanoribbons, Y-junction structures and ordered hexagonal holes. Individual graphene crystals and continuous films were grown on Cu foil using camphor as solid source in an AP-CVD technique. Highly anisotropic etching was observed with a gas mixture of H<sub>2</sub> and Ar (98:2 sccm) annealing at a temperature of 1000 °C. The etching constantly enhanced with increase in annealing duration and eventually erasing significant part of graphene on Cu foil. The controlled etching process is quite significant as the nanoribbons, Y-junction and other graphene structures were formed with clear edges. The pronounced graphene edges of individual ribbons created 120° to form a Y-shape structure. Formation of nanoribbons with interconnection of two larger graphene domains was also observed, however width of the fabricated nanoribbons was not uniform. Thus, our finding shows that controllable anisotropic etching of graphene can be achieved to fabricate particular graphene structures with preferential edges for electronic device applications.

### **Acknowledgements**

The work is supported by the funds for the development of human resources in science and technology, Japan. The authors RP, SS and GK have equally contributed in this work.

## References

1. A. K. Geim and K. S. Novoselov, *Nat. Mater.*, 2007, 6, 183.
2. K. S. Novoselov, A. K. Geim, S. V. Morozov, D. Jiang, M. I. Katsnelson, I. V. Grigorieva, S. V. Dubonos and A. A. Firsov, *Nature*, 2005, 438, 197.
3. Y. Zhang, Y.-W. Tan, H. L. Stormer and P. Kim, *Nature*, 2005, 438, 201.
4. S. Morozov, K. Novoselov, M. Katsnelson, F. Schedin, D. C. Elias, J. A. Jaszczak and A. K. Geim, *Phys. Rev. Lett.*, 2008, 100, 016602.
5. A. S. Mayorov, R. V. Gorbachev, S. V. Morozov, L. Britnell, R. Jalil and L. A. Ponomarenko, *Nano lett.*, 2011, 11, 2396.
6. F. Schwierz, *Nat. Nanotechnol.*, 2010, 5, 487.
7. K.S. Novoselov, V.I. Fal'ko, L. Colombo, P.R. Gellert, M.G. Schwab and K. Kim, *Nature*, 2012, 490, 192.
8. L. Tapasztó, G. Dobrik, P. Lambin and L.P. Biró, *Nat. Nanotechnol.*, 2008, 3, 397.
9. K. Nakada, M. Fujita, G. Dresselhaus and M. S. Dresselhaus, *Phys. Rev. B.*, 1996, 54, 17954.
10. M. Y. Han, B. Özyilmaz, Y. Zhang and P. Kim, *Phys. Rev. Lett.*, 2007, 98, 206805.
11. Y.-M. Lin, V. Perebeinos, Z. Chen and P. Avouri, *Phys. Rev. B*, 2008, 78, 161409R.
12. L. Ma, J. Wang and F. Ding, *ChemPhysChem*, 2013, 14, 47.

13. Y.-W. Son, M. L. Cohen and S. G. Louie, *Phys. Rev. Lett.*, 2006, 97, 216803.
14. Y. -W. Son, M. L. Cohen and S. G. Louie, *Nature*, 2006, 444, 347.
15. Z. Chen, Y. M. Lin, M. J. Rooks and P. Avouris, *Physica E*, 2007, 40, 228.
16. K. A. Ritter and J. W. Lyding, *Nat. Mater.*, 2009, 8, 235.
17. J. M. Tour, *Chem. Mater.*, 2014, 26, 163.
18. J. Cai, P. Ruffieux, R. Jaafar, M. Bieri, T. Braun, S. Blankenburg, M. Muoth, A. P. Seitsonen, M. Saleh, X. Feng, K. Müllen and R. Fasel, *Nature*, 2010, 466, 470.
19. G. -X. Ni, Y. Zheng, S. Bae, H.R. Kim, A. Pachoud, Y.S. Kim, C. L. Tan, D. Im, J. H. Ahn, B. H. Hong and B. Ozyilmaz, *ACS Nano.*, 2012, 6, 115.
20. X. L. Li, X. R. Wang, L. Zhang, S. W. Lee and H. J. Dai, *Science*, 2008, 319, 1229.
21. L. Y. Jiao, L. Zhang, X. R. Wang, G. Diankov and H. J. Dai, *Nature*, 2009, 458, 877.
22. L. Jiao, X. Wang, G. Diankov, H. Wang and H. Dai, *Nat. Nanotechnol.*, 2010, 5, 321.
23. D. V. Kosynkin, A. L. Higginbotham, A. Sinitskii, J. R. Lomeda, A. Dimiev, B. K. Price and J. M. Tour, *Nature*, 2009, 458, 872.
24. A. L. Elías, A. R. Botello-Méndez, D. Meneses-Rodríguez, V. J. González, D. Ramírez-González, L. Ci, E. M.Sandoval , P. M. Ajayan, H. Terrones and M. Terrones, *Nano Lett.*, 2009 10, 366.

25. X. Wang and H. Dai, *Nat. Chem.*, 2010, 2, 661.
26. L.C. Campos, V.R. Manfrinato, J.D. Sanchez-Yamagishi, J. Kong and P. Jarillo-Herrero, *Nano Lett.*, 2009, 9, 2600.
27. P. S. Fernández, K. Yoshida, Y. Ogawa, M. Tsuji and H. Ago, *Adv. Mater.*, 2013, 25, 6562.
28. R. Yang , L. Zhang , Y. Wang , Z. Shi , D. Shi , H. Gao, E. Wang and G. Zhang, *Adv. Mater.*, 2010, 22, 4014.
29. Y Zhang, Z Li, P. Kim, L. Zhang and C. Zhou, *ACS Nano*, 2012, 6, 126.
30. L. Ci, Z. Xu, L. Wang, W. Gao, F. Ding, K. F. Kelly, B. I. Yakobson and P. M. Ajayan *Nano Res.*, 2008, 1, 116.
31. P. Nemes-Incze, G. Magda, K. Kamaras and L. P. Biro, *Nano Res.*, 2010, 3, 110.
32. S. S. Datta, D. R. Strachan, S. M. Khamis and A. T. C. Johnson, *Nano Lett.*, 2008, 8, 1912.
33. D. Luo , F. Yang , X. Wang , H. Sun , D. Gao , R. Li, J. Yang and Y. Li, *Small*, 2014, 10, 2809.
34. H. Ago Y. Kayo, P. S.-Fernández, K. Yoshida and M. Tsuji, *Carbon*, 2014, 78, 339.
35. D. H. Jung, C. Kang, D. Yoon, H. Cheong and J. S. Lee, *Carbon*, 2015, 2015, 89, 242.

36. L. Zhu, J. Wang, T. Zhang, L. Ma, C. W. Lim, F. Ding and X. C. Zeng, *Nano Lett.*, 2010, 10, 494.
37. L. Ma, H. Hu, L. Zhu and J. Wang, *J. Phys. Chem. C*, 2011, 115, 6195.
38. G Zhang and H. Zhang, *Nanoscale*, 2011, 3, 4604.
39. Z. Lin. and W. Jun, *Chin. Phys. B*, 2014, 23, 087202.
40. A. N. Andriotisa and M. Menonb, *Appl. Phys. Lett.*, 2008, 92, 042115.
41. J. F. Liu, K and S. Chan, *J. Phys. Soc. Jpn.*, 2013, 82, 074711.
42. W. F. Tsai, C. Y. Huang, T. R. Chang, H. Lin, H. T. Jeng and A. Bansilature, *Nat. Commun.*, 2012, 4, 1500.
43. S. Sharma, G. Kalita, R. Hirano, S. M. Shinde, R. Papon, H. Ohtani and M. Tanemura, *Carbon*, 2014, 72, 66
44. L. Liu, J. Park, D. A. Siegel, K. F. McCarty, K. W. Clark, W.n Deng, L. Basile, J. C. Idrobo, A. P. Li and G. Gu, *Science*, 2014, 43, 163.
45. N. Gothard, C. Daraio, J. Gaillard, R. Zidan, S. Jin and A. M. Rao, *Nano Lett.*, 2004, 4, 213.

**Figure captions**

**Figure 1** (a) and (b) optical microscope images of graphene crystals grown from solid camphor precursor by AP-CVD process. (c) Raman spectra of the synthesized graphene on Cu foil.

**Figure 2** optical microscope images (a) and (b) of the etched graphene sample by annealing at 1000 °C in the atmosphere of Ar:H<sub>2</sub> gas mixture; (c) etched graphene crystal with formation of a well-defined hexagonal hole. (d) Raman spectra of the etched graphene and partially oxidized Cu surface.

**Figure 3** FE-SEM images of (a) etched graphene sample, presenting various structures with pronounced edges. FE-SEM images of (b) and (c) graphene edges with 60° and 120°, indicating etching along symmetric directions of the graphene lattice.

**Figure 4** (a) FE-SEM image corresponding to back scattered electron (BSE) providing compositional contrast. We observed SiO<sub>2</sub> nanoparticles as bright contrast inside the hole in graphene crystals and etched areas. (b) FE-SEM, (c) and (d) elementary mapping for carbon and oxygen. (e) Selective AES analysis of the etched graphene structure on Cu foil.

**Figure 5** FE-SEM images of (a) an ordered etched hexagonal hole as well as ribbon like graphene structure, (b) formation of Y-shape graphene ribbons structure with edge etching (three ribbons form  $120^{\circ}$  to each other), (c) and (d) nanoribbon structure with the etching process on Cu foil. The nanoribbon is formed with interconnection of two larger graphene domains.

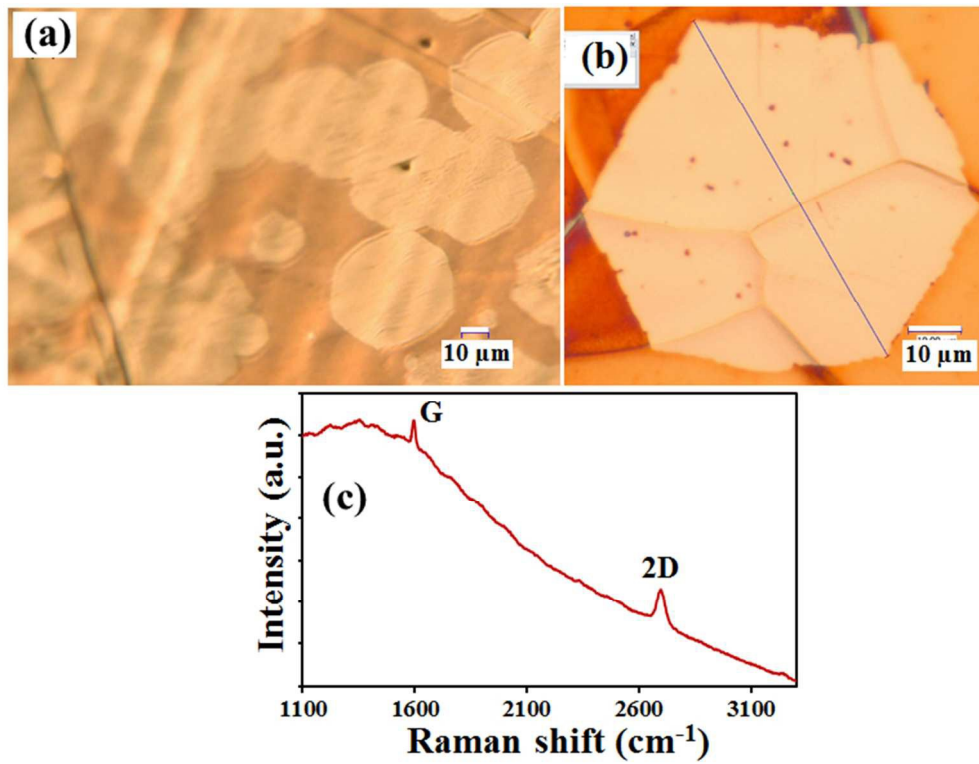


Figure 1

205x183mm (96 x 96 DPI)

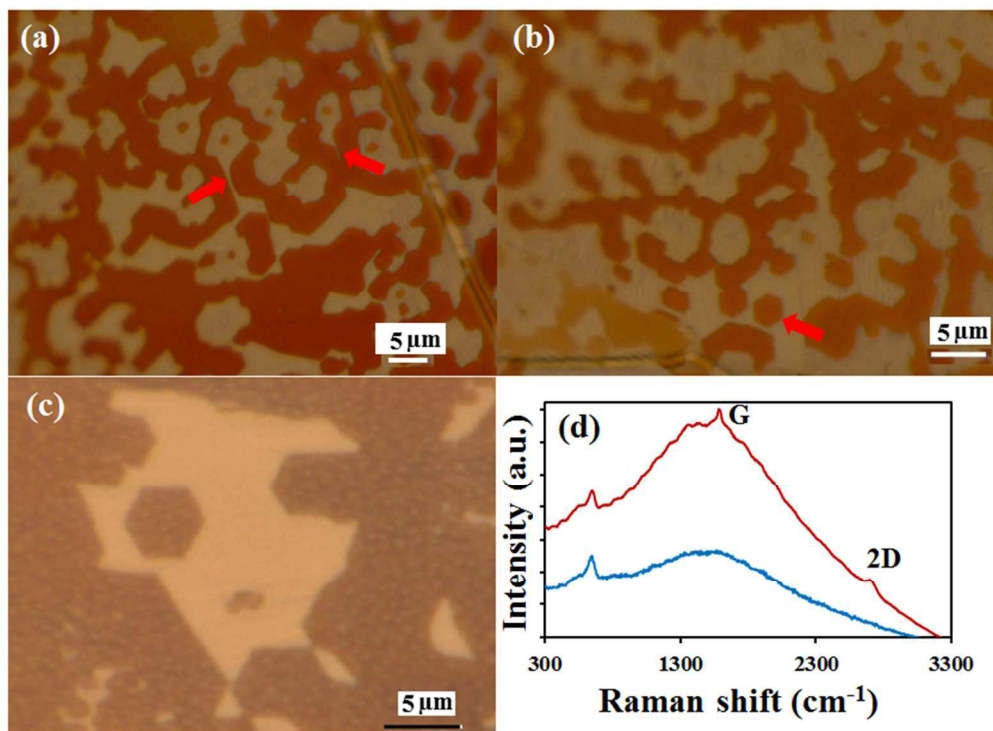
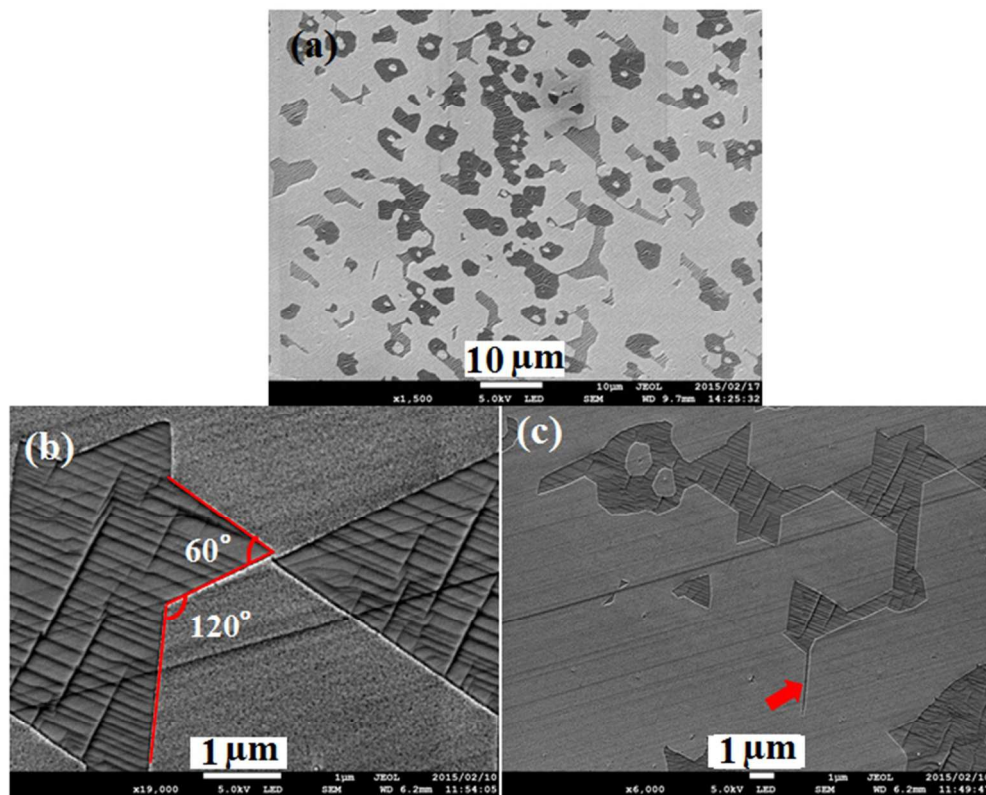


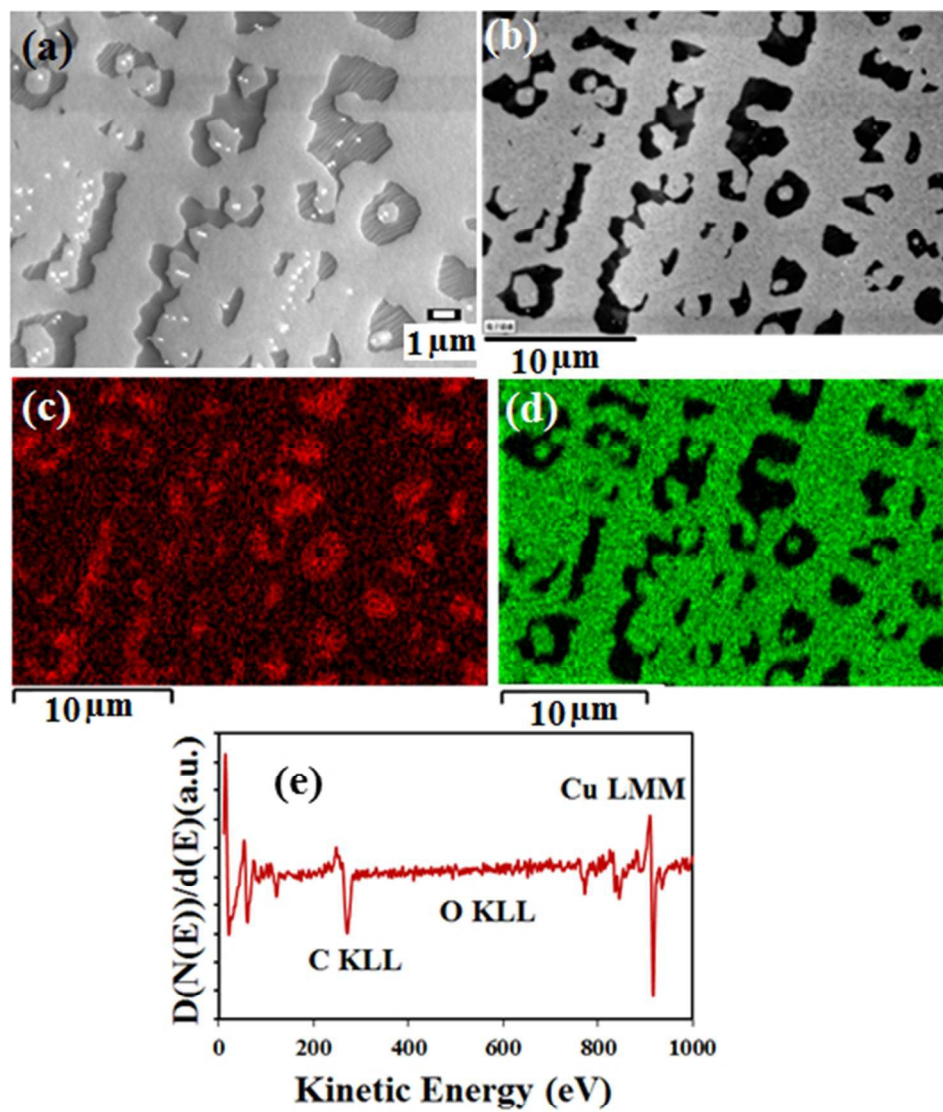
Figure 2

222x192mm (96 x 96 DPI)



**Figure 3**

186x171mm (96 x 96 DPI)

**Figure 4**

134x170mm (96 x 96 DPI)

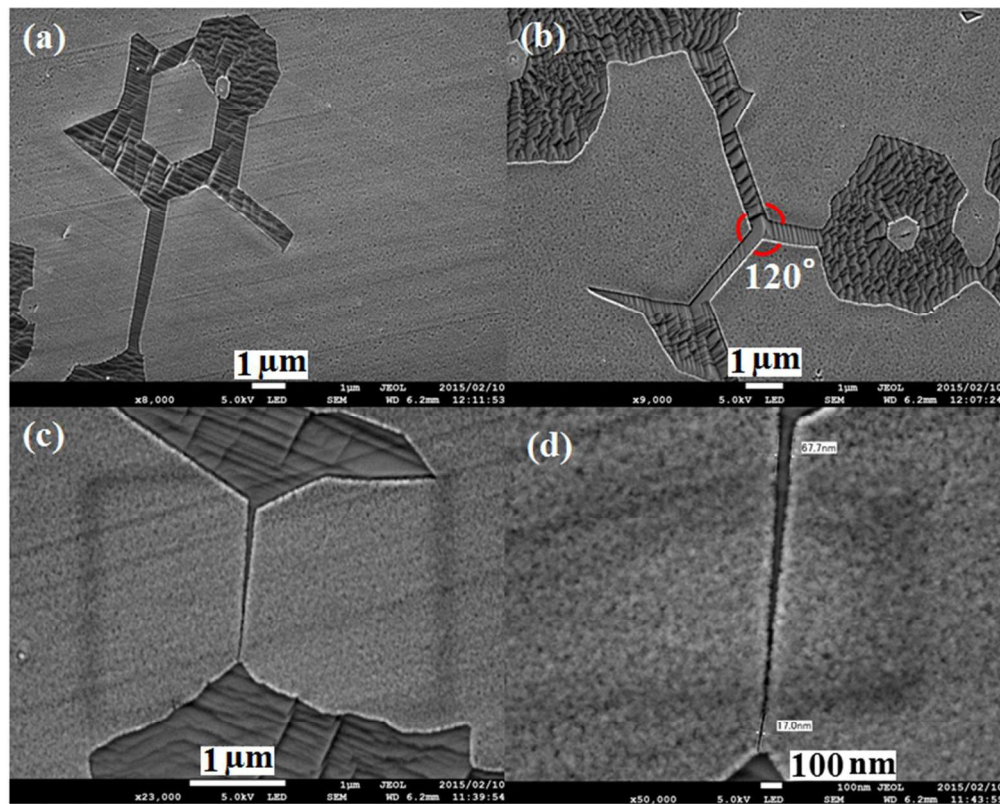


Figure 5

205x187mm (96 x 96 DPI)